

# Quantum spin Hall effect protected by spin $U(1)$ quasi-symmetry

Lu Liu,<sup>1,2,\*</sup> Yuntian Liu,<sup>1,\*</sup> Jiayu Li,<sup>1</sup> Hua Wu,<sup>2,3,4</sup> and Qihang Liu<sup>1,5,†</sup>

<sup>1</sup>*Department of Physics and Shenzhen Institute for Quantum Science and Engineering (SIQSE), Southern University of Science and Technology, Shenzhen 518055, China*

<sup>2</sup>*Laboratory for Computational Physical Sciences (MOE), State Key Laboratory of Surface Physics, and Department of Physics, Fudan University, Shanghai 200433, China*

<sup>3</sup>*Shanghai Qi Zhi Institute, Shanghai 200232, China*

<sup>4</sup>*Collaborative Innovation Center of Advanced Microstructures, Nanjing 210093, China*

<sup>5</sup>*Guangdong Provincial Key Laboratory of Computational Science and Material Design, Southern University of Science and Technology, Shenzhen 518055, China*

(Dated: February 22, 2024)

Quantum spin Hall (QSH) effect, where electrons with opposite spin channels are deflected to opposite sides of a two-dimensional system with a quantized conductance, was believed to be characterized by a nontrivial topological index  $Z_2$ . However, spin mixing effects in realistic materials often lead to deviation of the spin Hall conductance from exact quantization. In this Letter, we present a universal symmetry indicator for diagnosing QSH effect in realistic materials, termed spin  $U(1)$  quasi-symmetry. Such a symmetry eliminates the first-order spin-mixing perturbation and thus protects the near-quantization of SHC, applicable to time-reversal-preserved cases with either  $Z_2 = 1$  or  $Z_2 = 0$ , as well as time-reversal-broken scenarios. We propose that spin  $U(1)$  quasi-symmetry is hidden in the subspace spanned by the doublets with unquenched orbital momentum and emerges when SOC is present, which can be realized in 19 crystallographic point groups. Particularly, we identify a previous overlooked even spin Chern phase with a trivial  $Z_2$  index as an ideal platform for achieving a near-double-quantized SHC, as exemplified by twisted bilayer transition metal dichalcogenides and monolayer  $\text{RuBr}_3$ . Our work offers a new perspective for understanding QSH effect and significantly expands the material pool for the screening of exemplary material candidates.

**Introduction.**—Two-dimensional (2D) quantum spin Hall (QSH) insulators manifest a plateau of spin Hall conductance (SHC) with a nearly quantized value inside the energy gap of the bulk. They have triggered the recent prosperity of topological phases of matter and topological electronics owing to their promising potential dissipationless spin transports [1–8]. Conventional QSH insulators are diagnosed by a nontrivial  $Z_2$  index as the symmetry indicator, protected by time-reversal symmetry (TRS) [2], and are expected to exhibit quantized SHC. However, it has come to light recently that certain  $Z_2 = 1$  QSH insulators manifest significant deviations from the expected quantized value  $ne/2\pi$ , where  $n$  is an integer and  $e$  stands for electron charge [9–12]. More intriguingly, experiments have observed two pairs of helical edge states and near-quantized conductance in twisted bilayer  $\text{WSe}_2$  within the  $Z_2 = 0$  regime [13, 14]. In addition, recent observations also reveal the helical edge state in antiferromagnetic  $\text{FeSe}$  monolayer [15, 16]. These findings indicate that while the  $Z_2$  index and gapless edge states are destroyed by spin mixing, the QSH effects may not be severely affected.

Generically, quantized SHC is calculated by  $\sigma_{xy}^S = C_S \frac{e}{2\pi}$  [17], where the spin Chern number  $C_S$ , defined by the difference between the Chern numbers of spin-up and spin-down channels, serves as a topological invariant [17–19]. However, it is notable that the ‘spin’ in  $C_S$  is

uniquely defined for each wavevector  $\mathbf{k}$  in the Brillouin zone if spin-mixing interactions exist. When considering the collective behavior of all the  $\mathbf{k}$  points, e.g., SHC, the real spin is no longer a good quantum number [2, 17–20]. Therefore, only when the real-spin-component  $S_z$  is preserved, corresponding to a  $U(1)$  spin rotation symmetry, SHC becomes exactly quantized [2, 17, 20, 21]. In realistic materials, however, this condition cannot be met due to intrinsic spin-orbit coupling (SOC) and orbital hybridization. This leads to a crucial question: how can the near-quantized SHC plateau emerging from the bulk gap of a 2D material, which can be a compromised definition of QSH effect, be protected and understood by symmetry? Several studies have sought to unravel the factors influencing QSH effect. For instance, Rashba SOC has been demonstrated to be destructive to QSH effect, arising from the breakdown of in-plane mirror symmetry [1, 2, 20]. Moreover, high in-plane symmetry has been suggested to enhance the potential for near-quantization feature via comparisons among QSH insulators with hexagonal, square, and rectangular lattices [12]. Furthermore, the dependence of SHC values on the spin axis has also been investigated [11, 22, 23]. Yet, an effective symmetry indicator for QSH effect remains elusive.

In this Letter, we show that besides a nontrivial  $C_S$ , there is a previous overlooked symmetry indicator for the diagnosis of QSH effect, namely spin  $U(1)$  quasi-symmetry. The significance of such an approximate symmetry is to eliminate the first-order spin-mixing interactions, thereby protecting the near-quantization of SHC.

\* Lu Liu and Yuntian Liu contributed equally to this work.

† Corresponding author. liuqh@sustech.edu.cn

We propose that the spin  $U(1)$  quasi-symmetry is inherently hidden in the subspace formed by the states possessing unquenched orbital angular momentum  $l_z$ , and emerges when SOC is present. Such states are characterized by 1D complex irreducible representations (irreps) and 2D irreps supported in 19 crystallographic point groups. Interestingly, we identify an even spin Chern (ESC) phase with a trivial  $Z_2$  index but a non-trivial  $C_S$  and spin  $U(1)$  quasi-symmetry as an ideal platform to realize high near-quantized SHC. By symmetry analysis and first-principles calculations, we provide design principles for such ESC insulators, exemplified by twisted bilayer transition metal dichalcogenides (TMDs) and  $\text{RuBr}_3$  monolayer. Furthermore, we also apply our theory to antiferromagnetic FeSe monolayer, demonstrating that near-quantized SHC could appear even in TRS-broken systems with spin  $U(1)$  quasi-symmetry.

**Spin  $U(1)$  quasi-symmetry.**— Quasi-symmetry was originally introduced to account for the near degeneracies and the resultant large Berry curvature in CoSi [24, 25]. Later, a generic theory on quasi-symmetry was developed, expanding the conventional group theory to address questions regarding large-or-small splittings [26]. Specifically, quasi-symmetry describes the hidden symmetry within a specific degenerate eigensubspace under the unperturbed Hamiltonian  $H_0$ , thereby forming an enlarged group beyond the symmetry group of  $H_0$  (denoted as  $\mathcal{G}_{H_0}$ ) [26]. Importantly, the presence of quasi-symmetry constrains the symmetry-lowering interactions  $H'$  to operate only as a second-order effect. For instance, the subspace formed by the doubly degenerate spin eigenstates,  $|\uparrow\rangle$  and  $|\downarrow\rangle$ , is invariant under spin  $U(1)$  symmetry operator  $e^{i\theta\sigma_z}$ . When adding a spin-mixing interaction  $H'$ , the term  $\langle\uparrow|H'|\downarrow\rangle$ , if invariant under all operations in  $\mathcal{G}_{H_0}$ , is allowed to be non-zero as a first-order perturbation effect. However, the inherent spin  $U(1)$  symmetry within the spin eigensubspace gives that

$$\langle\uparrow|H'|\downarrow\rangle \xrightarrow{e^{i\theta\sigma_z}} \langle\uparrow|e^{i\theta\sigma_z}H'(e^{i\theta\sigma_z})^{-1}|\downarrow\rangle = e^{i2\theta}\langle\uparrow|H'|\downarrow\rangle. \quad (1)$$

The presence of the phase factor  $e^{i2\theta}$  enforces  $\langle\uparrow|H'|\downarrow\rangle = 0$ , suggesting that  $H'$  acts in the second-order perturbation. Therefore, while excluded from  $\mathcal{G}_{H_0}$ , the spin  $U(1)$  symmetry exists as a quasi-symmetry within the subspace spanned by  $\{|\uparrow\rangle, |\downarrow\rangle\}$ , and significantly, it eliminates the first-order spin-mixing perturbation, which is a dominant detriment to the quantization in QSH phase.

An important subsequent step is to identify the conditions that cause spin  $U(1)$  quasi-symmetry in real materials. The key point is to ensure that within an eigensubspace that is invariant under  $e^{i\theta\sigma_z}$ , the spin-mixing term merely acts as a perturbation relative to the spin-preserving term. We propose that such conditions are satisfied by utilizing the states with unquenched orbital angular momentum  $l_z$ . The simplest case is a spin-degenerate band in nonmagnetic materials. As shown in Fig. 1(a), in the spin doublet

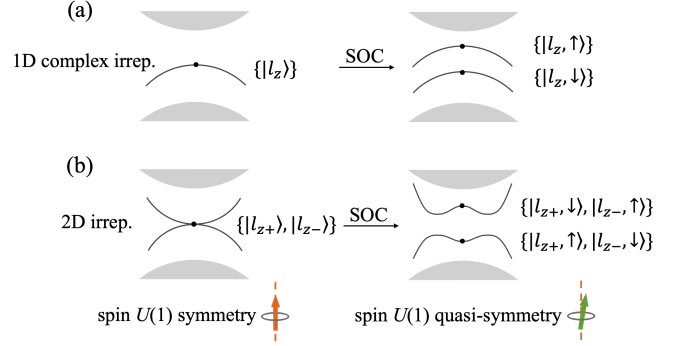


FIG. 1. Schematic of the spin  $U(1)$  quasi-symmetry and its design principles: Spin  $U(1)$  quasi-symmetry is hidden in the subspace formed by the states with nonzero  $l_z$ , which is allowed by (a) the spin doublet characterized by 1D complex irreps and (b) the orbital doublet characterized by 2D irreps, and emerges when SOC is present.

$\{|l_z, \uparrow\rangle, |l_z, \downarrow\rangle\}$ , the spin-preserving SOC matrix elements  $\langle l_z, \uparrow | \sigma_z L_z | l_z, \uparrow \rangle = l_z$  and  $\langle l_z, \downarrow | \sigma_z L_z | l_z, \downarrow \rangle = -l_z$  are non-vanishing. In contrast, the spin-mixing SOC elements  $\langle l_z, \uparrow | \sigma_x L_x + \sigma_y L_y | l_z, \downarrow \rangle$  are zero unless involving remote bands to invoke a second-order effect. Therefore, around the  $\mathbf{k}$  points where little point groups support such doublets and when SOC emerges, spin-mixing SOC  $\sigma_{x,y} L_{x,y}$  is effectively a second-order perturbation compared to the dominant spin-preserving SOC  $\sigma_z L_z$ . Upon projecting the Hamiltonian onto the subspace expanded by  $\{|l_z, \uparrow\rangle, |l_z, \downarrow\rangle\}$ , the unperturbed Hamiltonian  $H_0$  and the perturbed Hamiltonian  $H'$  can be written as  $H_0 \sim \sigma_z h_0(\mathbf{k})$  and  $H' \sim \sigma_{x,y} h'(\mathbf{k})$ , respectively. Indeed, under the action of spin  $U(1)$  symmetry operator  $e^{i\theta\sigma_z}$ ,  $H_0$  remains invariant, whereas  $H'$  does not. Fig. 1(a) represents the bands with unquenched  $l_z$  at non time-reversal-invariant momenta, such as the top valance bands near the  $K$  valley in  $H$ -TMDs [27].

The spin-preserving SOC also dominates when the subspace is spanned by an orbital doublet, as depicted in Fig. 1(b). Therefore, with SOC the subspace is formed by  $\{|\uparrow\rangle, |\downarrow\rangle\} \otimes \{|l_{z+}\rangle, |l_{z-}\rangle\}$ , where  $l_{z\pm}$  denotes opposite orbital angular momentum. In this case, the unperturbed Hamiltonian  $H_0$  and the perturbed Hamiltonian  $H'$  take the form of  $H_0 \sim \sigma_z \otimes [\tau_z + h_0(\mathbf{k})\tau_{x,y,z}]$  and  $H' \sim \sigma_{x,y} \otimes h'(\mathbf{k})\tau_{x,y,z}$ , respectively, where  $\sigma/\tau$  denotes Pauli matrices for spin/orbital degrees of freedom. Therefore, spin  $U(1)$  symmetry emerges as a quasi-symmetry of the subspace spanned by the states with nonzero  $l_z$ .

Regarding the symmetry requirement, the spin doublet carrying nonzero  $l_z$  in Fig. 1(a) is characterized by 1D complex irreps. This condition is satisfied by 8 crystallographic point groups:  $(C_3, C_{3h}, C_4, S_4, C_{4h}, C_6, S_6, C_{6h})$ . The orbital doublet shown in Fig. 1(b) is supported by 11 point groups  $(C_{3v}, D_3, D_{3d}, D_{3h}, C_{4v}, D_4, D_{2d}, D_{4h}, C_{6v}, D_6, D_{6h})$  with 2D irreps and the abovementioned 8 groups with conjugate 1D complex irreps in TRS-

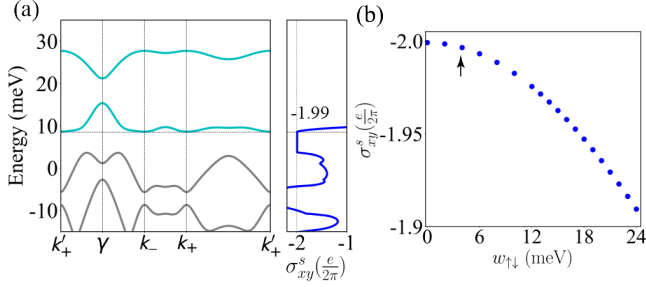


FIG. 2. (a) Moiré band structure at a twist angle of  $2.5^\circ$ . The top two bands are indicated in green curves. The energy dependence of SHC is plotted in the right panel. (b) SHC values as a function of the spin-mixing strength  $w_{\uparrow\downarrow}$ . The arrow marks the  $w_{\uparrow\downarrow}$  value of 6 meV used in (a).

preserved systems. Consequently, there are in total 19 crystallographic point groups supporting the states with nonzero  $l_z$  and thus spin  $U(1)$  quasi-symmetry. Note that a similar approach can be directly extended to magnetic materials, which will be discussed later.

It is worth noting that our discussions about spin  $U(1)$  quasi-symmetry is not confined to  $Z_2 = 1$  or  $Z_2 = 0$  cases. In fact, the spin-mixing terms induced by symmetry breaking could also weaken the SHC in the  $Z_2 = 1$  conventional QSH insulators, as demonstrated in previous studies [1, 2, 12, 20]. Therefore, for these  $Z_2 = 1$  systems, spin  $U(1)$  quasi-symmetry which eliminates the first-order spin-mixing perturbation still plays a crucial role for protecting the near-quantization. In the following section, we present two types of  $Z_2 = 0$  spin Chern insulators with spin  $U(1)$  quasi-symmetry and show that such a topological phase manifests a high and near-quantized SHC plateau, rendering an ideal platform for observing QSH effects.

**Twisted bilayer TMDs: Spin doublet.**— We next provide a realistic example of ESC insulators with spin  $U(1)$  quasi-symmetry promoted by the spin doublet [Fig. 1(a)]: twisted bilayer TMDs, in which the moiré valence bands are formed from the states at the  $\pm K$  valleys of two  $H$ -TMD monolayers. Although individual  $H$ -TMD monolayers do not exhibit QSH effect [28], moiré bands in twisted bilayers have been theoretically predicted and experimentally confirmed to manifest a nontrivial ESC phase [13, 14, 29, 30]. Here we emphasize that while the nontrivial  $C_S$  is caused by the moiré structure, the observed QSH effects also benefit from the spin  $U(1)$  quasi-symmetry hidden in the electronic structure of each  $H$ -TMD monolayer. For  $H$ -TMD monolayers, the topmost valence states at  $+K$ -valley with little point group  $C_{3h}$  consist of spin doublet  $\{|l_z = +2, \uparrow\rangle, |l_z = +2, \downarrow\rangle\}$  [27] when SOC is absent, in excellent agreement with the symmetry requirement of Fig. 1(a). To see the role of spin  $U(1)$  quasi-symmetry in twisted bilayer TMDs, we adopt the continuum model Hamiltonian at  $+K$  valley and consider both spin-preserving and spin-mixing effects by including the  $\{|l_z = +2, \uparrow\rangle$  and  $|l_z = +2, \downarrow\rangle\}$  states,

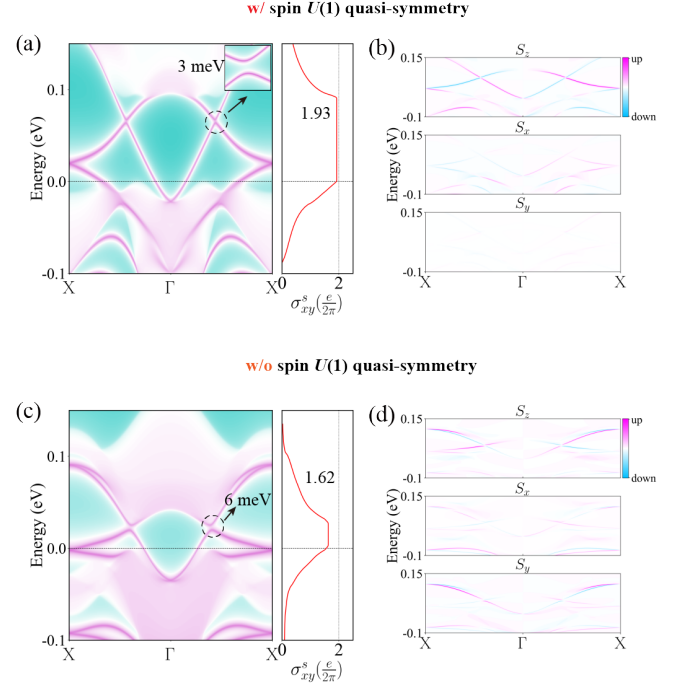


FIG. 3. (a, c) The edge states and SHC, and (b, d) spin components of the edge states in RuBr<sub>3</sub> monolayer. The undistorted structure is adopted in (a-b), in which spin  $U(1)$  symmetry is present in the low-energy states. In contrast, the crystal structure in (c-d) undergoes a deformation to a low-symmetry phase under a uniaxial tensile strain, resulting in the absence of spin  $U(1)$  symmetry. The Fermi level is indicated as the dashed lines.

see details in Supplementary Section S1 [31]. When SOC emerges, the spin degeneracy at  $+K$  is lifted, resulting in a strong spin-preserving SOC gap ( $\sim 200$  meV [29]) between the  $|l_z = +2, \uparrow\rangle$  band and the  $|l_z = +2, \downarrow\rangle$  band.

We calculate the moiré band structure at a twist angle of  $2.5^\circ$ . As shown in Fig. 2(a), the top two bands are well separated from the third band. By integrating the Berry curvature within the first moiré Brillouin zone, we find that the first two moiré bands at  $+K$  valley possess a nontrivial Chern number of  $-2$ . Due to spin-valley locking in TMDs, the  $-K$  valley must carry a Chern number of 2. Therefore, the twisted bilayer is in an ESC phase with  $|C_S| = 2$ . Moreover, our calculations on SHC reveal a plateau within the energy gap between the second and third bands corresponding to the moiré hole filling factor  $\nu = 4$ , as shown in the right panel of Fig. 2(a). Notably, the SHC value of  $-1.99$  closely approaches the quantized value of  $-2$ . This is attributed to the essential role of spin  $U(1)$  quasi-symmetry eliminating the first-order perturbation of spin-mixing interaction [31], i.e.,  $\langle l_z = +2, \uparrow | H' | l_z = +2, \downarrow \rangle = 0$ . Furthermore, we show that due to that spin-mixing effects act at most a second-order perturbation, even increasing the spin-mixing strength to larger than 20 meV, the SHC value remains high and nearly quantized to  $-2$ . Therefore, we conclude that  $|C_S| = 2$  and spin  $U(1)$  quasi-

symmetry, which originates from the moiré band renormalization and the spin doublets with unquenched  $l_z$  for a monolayer, respectively, are both indispensable factors to ensure the near-quantized SHC successfully observed in twisted bilayer TMDs [13, 14].

**RuBr<sub>3</sub> monolayer: Orbital doublet.**—Next, we introduce another example of ESC insulators with spin  $U(1)$  quasi-symmetry supported by orbital doublet: the RuBr<sub>3</sub> monolayer. The monolayer has a space group  $P\bar{3}1m$ , with the little point group  $D_{3d}$  at the  $\Gamma$  point, as shown in Fig. 1(b). As shown in Fig. S2(a), the orbital doublet  $\{|e'_+\rangle, |e'_-\rangle\}$  governs the low-energy physics of RuBr<sub>3</sub>. This degeneracy is lifted by introducing SOC effects, and a bulk gap of about 100 meV is opened. Notably, the onsite first-order spin-preserving SOC contributes a significant gap of larger than 300 meV at  $\Gamma$  point. To investigate the topological nature of RuBr<sub>3</sub> monolayer, we first calculate the  $Z_2$  index by computing the parity eigenvalues of valence bands at the time-reversal-invariant momenta [32]. The same parity at  $\Gamma$  and M results in  $Z_2 = 0$ , suggesting that RuBr<sub>3</sub> is a  $Z_2$  trivial insulator. Interestingly, despite RuBr<sub>3</sub> belongs to the  $Z_2 = 0$  phase, its nontrivial topological features are evident in the edge spectrum and SHC. As shown in Fig. 3(a) and (b), RuBr<sub>3</sub> exhibits two pairs of helical edge states and two Dirac-like edge crossings with tiny gaps of 3 meV. Furthermore, the SHC plateau of RuBr<sub>3</sub> persists within the bulk gap, and its value of 1.93 closely approximates the quantized value of 2. Through adiabatically restoring the spin  $U(1)$  symmetry [18, 19, 33] and calculating the  $C_S$ , we confirm that RuBr<sub>3</sub> monolayer is in an ESC phase characterized by  $C_S = 2$ , see Supplementary Section S3 [31].

Here we construct an effective model Hamiltonian around the  $\Gamma$  point to capture the topological nature and the quasi-symmetry of RuBr<sub>3</sub>. The generators of little point group  $D_{3d}$  at  $\Gamma$  point are three-fold rotation symmetry  $C_{3z}$  along the  $z$  axis, two-fold rotation symmetry  $C_{2y}$  along the  $y$  axis, and space inversion symmetry  $I$ . In the basis of  $\{|e'_+, \uparrow\rangle, |e'_-, \uparrow\rangle, |e'_+, \downarrow\rangle, |e'_-, \downarrow\rangle\}$ , the representation matrices of the symmetry operations are given by  $C_{3z} = e^{i\frac{2\pi}{3}\sigma_z} \otimes e^{-i\frac{2\pi}{3}\tau_z}$ ,  $C_{2y} = e^{i\frac{\pi}{2}\sigma_y} \otimes \tau_x$ ,  $I = \mathbb{I}_{2 \times 2} \otimes -\mathbb{I}_{2 \times 2}$ , and TRS  $T = \mathcal{K} \cdot i\sigma_y \otimes \tau_x$ , where  $\mathcal{K}$  is the complex conjugation operator and  $\mathbb{I}_{2 \times 2}$  is a  $2 \times 2$  identity matrix. By imposing those symmetries, we derive the generic form of the effective Hamiltonian  $H(\mathbf{k})$  as follows:

$$\begin{aligned} H(\mathbf{k}) &= H_0(\mathbf{k}) + H'(\mathbf{k}) \\ H_0(\mathbf{k}) &= \epsilon_0(\mathbf{k})\mathbb{I}_{4 \times 4} + C[(k_x^2 - k_y^2)\sigma_0 \otimes \tau_x - 2k_x k_y \sigma_0 \otimes \tau_y] \\ &\quad + D(k_x^2 + k_y^2)\sigma_z \otimes \tau_z + E\sigma_z \otimes \tau_z \\ H'(\mathbf{k}) &= F[(k_x^2 - k_y^2)\sigma_x \otimes \tau_z + 2k_x k_y \sigma_y \otimes \tau_z] \end{aligned} \quad (2)$$

where  $\epsilon_0(\mathbf{k}) = A - B(k_x^2 + k_y^2)$ . For a negative  $E$ , this model describes the system in a nontrivial ESC phase with  $C_S = 2$ . Notably, within the subspace formed by

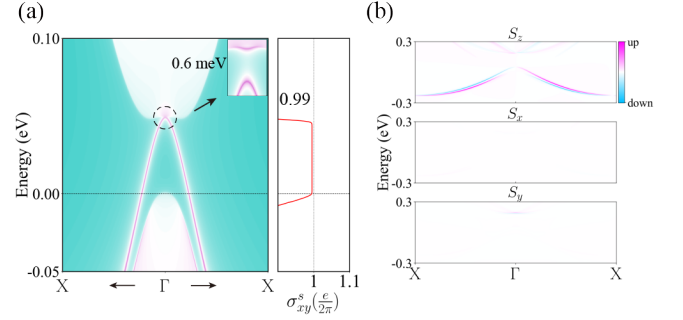


FIG. 4. (a) The edge states and SHC, and (b) the spin components of edge states in FeSe monolayer.

orbital doublet and electron spin, spin-mixing interaction is merely a perturbation compared to the dominant spin-preserving SOC effect. Here, the spin  $U(1)$  symmetry is present in the eigenspace of the unperturbed Hamiltonian  $H_0$  in Eq. (2), and it eliminates the first-order perturbation effect of  $H'$ , i.e.,  $\langle \uparrow | H' | \downarrow \rangle = 0$ , thereby protecting the QSH effect. This is verified by our DFT-calculated results: (i) a relatively small edge gap of 3 meV induced by second-order spin-mixing perturbation; (ii) the predominance of the spin-preserved  $S_z$  component in the edge states; (iii) a persistent SHC plateau within the bulk gap, with a value of 1.93, closely approximating the quantized value of 2, as shown in Figs. 3(a) and (b).

To further validate our theory, we apply a uniaxial tensile strain to break the spin  $U(1)$  quasi-symmetry in RuBr<sub>3</sub>. Specifically, the strain reduces the little group of the  $\Gamma$  point from  $D_{3d}$  to  $C_i$ , eliminating the orbital doublet and the spin  $U(1)$  quasi-symmetry, see Fig. S2(c). As illustrated by the comparisons between Figs. 3(a, b) and (c, d), the breakdown of spin  $U(1)$  quasi-symmetry leads to a considerable decrease in SHC values from 1.93 to 1.62, accompanied by an increase in the edge gap and enhanced spin-mixing  $S_{x,y}$  components in the edge states. Consequently, the essential role of spin  $U(1)$  quasi-symmetry in protecting the near-quantized SHC is verified.

**Antiferromagnetic FeSe monolayer.**— TRS-broken QSH insulators, which are out of  $Z_2$  classification, are also characterized by the spin Chern number  $C_S$  [19]. We clarify that, similar to the TRS-preserved cases, the near-quantization of SHC in TRS-broken QSH insulators not only requires a nonzero  $C_S$  but also necessitates the protection from spin  $U(1)$  quasi-symmetry. Here we focus on collinear antiferromagnetic configurations where the antiferromagnetic exchange interaction can be described by  $m\sigma_z \otimes \gamma_z$ , with  $\sigma$  and  $\gamma$  denoting the spin and site degrees of freedom, respectively, and  $m$  representing the magnitude of exchange splitting. Adding such a collinear antiferromagnetic order to the orbital doublet in Fig. 1(b), the unperturbed Hamiltonian  $H_0$  is simply extended by a direct product with  $m\gamma_z$ , thereby retaining the spin  $U(1)$  quasi-symmetry. Furthermore,



as detailed in Supplementary Section S5 [31], using the magnetic point group  $6'mm'$  as an example, we find that the absence of orbital doublets leads to the dominance of spin-mixing interactions. Therefore, we suggest that orbital doublets are also indispensable in collinear antiferromagnetic scenarios.

We next perform DFT calculations on antiferromagnetic monolayer FeSe, a recognized TRS-broken QSH insulator [15, 16, 34, 35], to validate our theory. In this  $C_S = 1$  system, the low-energy physics is governed by the orbital doublet  $\{l_{z+}, l_{z-}\}$ . Within such an eigenspace, the dominant SOC Hamiltonian is spin preserved rendering the first-order spin-mixing perturbation  $\langle \uparrow | H' | \downarrow \rangle = 0$ . Therefore, the eigenspace of FeSe manifests spin  $U(1)$  quasi-symmetry. Although TRS-breaking interactions inevitably introduces an edge gap, as shown in Fig. 4, the inherent spin  $U(1)$  quasi-symmetry, combined with significant exchange splitting [36], leads to a tiny edge gap of 0.6 meV and an almost quantized SHC of 0.99.

**Discussion.**— We clarify that while the exact spin  $U(1)$  symmetry does not exist in crystal solids, it can be approximately met accidentally in a case-specific manner. An example is the monolayer WTe<sub>2</sub>, where a persistent spin pattern forms at specific regions of the Brillouin zone [11, 22, 23]. However, such QSH insulators, dependent on specific chemical environments, can be hardly predicted or designed. Instead, spin  $U(1)$  quasi-symmetry, serving as a symmetry indicator, establishes a universal framework for predicting and elucidating QSH effect, linking topological invariants and symmetries to the long-sought near-quantized SHC. Notably, it bridges the gap between the widely acknowledged TRS-preserved  $Z_2 = 1$  QSH insulators and  $Z_2 = 0$  cases, as well as the TRS-broken QSH insulators. While  $Z_2$  invariant is irrelevant, the two indispensable prerequisites for QSH effect are spin  $U(1)$  quasi-symmetry and nontrivial  $C_S$ . Overall, our work provides a new perspective for understanding QSH effects and related topological phenomena, and greatly expands the potential material pool for the screening of “best-of-class” material candidates.

## ACKNOWLEDGEMENTS

We thank Quansheng Wu and Zhida Song for helpful discussions. Q. L. acknowledges support by National Key R&D Program of China under Grant No. 2020YFA0308900, National Natural Science Foundation of China under Grant No. 12274194, Guangdong Provincial Key Laboratory for Computational Science and Material Design under Grant No. 2019B030301001, Shenzhen Science and Technology Program under Grant No. RCJC20221008092722009, the Science, Technology and Innovation Commission of Shenzhen Municipality under Grant No. ZDSYS20190902092905285 and Center for Computational Science and Engineering of Southern Uni-

versity of Science and Technology.

- 
- [1] C. L. Kane and E. J. Mele, Quantum spin Hall effect in graphene, *Phys. Rev. Lett.* **95**, 226801 (2005).
  - [2] C. L. Kane and E. J. Mele,  $Z_2$  topological order and the quantum spin Hall effect, *Phys. Rev. Lett.* **95**, 146802 (2005).
  - [3] B. A. Bernevig, T. L. Hughes, and S.-C. Zhang, Quantum spin Hall effect and topological phase transition in HgTe quantum wells, *Science* **314**, 1757 (2006).
  - [4] M. König, S. Wiedmann, C. Brüne, A. Roth, H. Buhmann, L. W. Molenkamp, X.-L. Qi, and S.-C. Zhang, Quantum spin Hall insulator state in HgTe quantum wells, *Science* **318**, 766 (2007).
  - [5] M. Z. Hasan and C. L. Kane, Colloquium: Topological insulators, *Rev. Mod. Phys.* **82**, 3045 (2010).
  - [6] X.-L. Qi and S.-C. Zhang, Topological insulators and superconductors, *Rev. Mod. Phys.* **83**, 1057 (2011).
  - [7] I. Knez, R.-R. Du, and G. Sullivan, Evidence for helical edge modes in inverted InAs/GaSb quantum wells, *Phys. Rev. Lett.* **107**, 136603 (2011).
  - [8] W. Han, Y. Otani, and S. Maekawa, Quantum materials for spin and charge conversion, *npj Quant. Mater.* **3**, 1 (2018).
  - [9] Z. Fei, T. Palomaki, S. Wu, W. Zhao, X. Cai, B. Sun, P. Nguyen, J. Finney, X. Xu, and D. H. Cobden, Edge conduction in monolayer WTe<sub>2</sub>, *Nature Phys.* **13**, 677 (2017).
  - [10] S. Wu, V. Fatemi, Q. D. Gibson, K. Watanabe, T. Taniguchi, R. J. Cava, and P. Jarillo-Herrero, Observation of the quantum spin Hall effect up to 100 Kelvin in a monolayer crystal, *Science* **359**, 76 (2018).
  - [11] W. Zhao, E. Runburg, Z. Fei, J. Mutch, P. Malinowski, B. Sun, X. Huang, D. Pesin, Y.-T. Cui, X. Xu, J.-H. Chu, and D. H. Cobden, Determination of the spin axis in quantum spin Hall insulator candidate monolayer WTe<sub>2</sub>, *Phys. Rev. X* **11**, 041034 (2021).
  - [12] F. Matusalem, M. Marques, L. K. Teles, L. Matthes, J. Furthmüller, and F. Bechstedt, Quantization of spin Hall conductivity in two-dimensional topological insulators versus symmetry and spin-orbit interaction, *Phys. Rev. B* **100**, 245430 (2019).
  - [13] K. Kang, Y. Qiu, K. Watanabe, T. Taniguchi, J. Shan, and K. F. Mak, Observation of the double quantum spin Hall phase in moiré WSe<sub>2</sub>, (2024), [arXiv:2402.04196](#).
  - [14] K. Kang, B. Shen, Y. Qiu, K. Watanabe, T. Taniguchi, J. Shan, and K. F. Mak, Observation of the fractional quantum spin Hall effect in moiré MoTe<sub>2</sub>, (2024), [arXiv:2402.03294](#).
  - [15] Z. F. Wang, H. Zhang, D. Liu, C. Liu, C. Tang, C. Song, Y. Zhong, J. Peng, F. Li, C. Nie, L. Wang, X. J. Zhou, X. Ma, Q. K. Xue, and F. Liu, Topological edge states in a high-temperature superconductor FeSe/SrTiO<sub>3</sub>(001) film, *Nature Mater.* **15**, 968 (2016).
  - [16] Y. Yuan, W. Li, B. Liu, P. Deng, Z. Xu, X. Chen, C. Song, L. Wang, K. He, G. Xu, X. Ma, and Q.-K. Xue, Edge states at nematic domain walls in FeSe films, *Nano Lett.* **18**, 7176 (2018).
  - [17] D. N. Sheng, Z. Y. Weng, L. Sheng, and F. D. M. Haldane, Quantum spin-Hall effect and topologically invariant chern numbers, *Phys. Rev. Lett.* **97**, 036808 (2006).

- [18] E. Prodan, Robustness of the spin-charge number, *Phys. Rev. B* **80**, 125327 (2009).
- [19] Y. Yang, Z. Xu, L. Sheng, B. Wang, D. Y. Xing, and D. N. Sheng, Time-reversal-symmetry-broken quantum spin Hall effect, *Phys. Rev. Lett.* **107**, 066602 (2011).
- [20] L. Sheng, D. N. Sheng, C. S. Ting, and F. D. M. Haldane, Nondissipative spin Hall effect via quantized edge transport, *Phys. Rev. Lett.* **95**, 136602 (2005).
- [21] X.-G. Wen, Symmetry-protected topological phases in noninteracting fermion systems, *Phys. Rev. B* **85**, 085103 (2012).
- [22] J. H. Garcia, M. Vila, C.-H. Hsu, X. Waintal, V. M. Pereira, and S. Roche, Canted persistent spin texture and quantum spin Hall effect in WTe<sub>2</sub>, *Phys. Rev. Lett.* **125**, 256603 (2020).
- [23] C. Tan, M.-X. Deng, G. Zheng, F. Xiang, S. Albarakati, M. Algarni, L. Farrar, S. Alzahrani, J. Partridge, J. B. Yi, A. R. Hamilton, R.-Q. Wang, and L. Wang, Spin-momentum locking induced anisotropic magnetoresistance in monolayer WTe<sub>2</sub>, *Nano Letters* **21**, 9005 (2021).
- [24] C. Guo, L. Hu, C. Putzke, J. Diaz, X. Huang, K. Manna, F.-R. Fan, C. Shekhar, Y. Sun, C. Felser, C. Liu, B. A. Bernevig, and P. J. W. Moll, Quasi-symmetry-protected topology in a semi-metal, *Nat. Phys.* **18**, 813 (2022).
- [25] L.-H. Hu, C. Guo, Y. Sun, C. Felser, L. Elcoro, P. J. W. Moll, C.-X. Liu, and B. A. Bernevig, Hierarchy of quasi-symmetries and degeneracies in the CoSi family of chiral crystal materials, *Phys. Rev. B* **107**, 125145 (2023).
- [26] J. Li, A. Zhang, Y. Liu, and Q. Liu, Group theory on quasi-symmetry and protected near degeneracy, [arXiv:2311.12738](https://arxiv.org/abs/2311.12738) (2023).
- [27] D. Xiao, G.-B. Liu, W. Feng, X. Xu, and W. Yao, Coupled spin and valley physics in monolayers of MoS<sub>2</sub> and other group-VI dichalcogenides, *Phys. Rev. Lett.* **108**, 196802 (2012).
- [28] M. Costa, B. Focassio, L. M. Canonico, T. P. Cysne, G. R. Schleder, R. B. Muniz, A. Fazzio, and T. G. Rappoport, Connecting higher-order topology with the orbital hall effect in monolayers of transition metal dichalcogenides, *Phys. Rev. Lett.* **130**, 116204 (2023).
- [29] F. Wu, T. Lovorn, E. Tutuc, I. Martin, and A. H. MacDonald, Topological insulators in twisted transition metal dichalcogenide homobilayers, *Phys. Rev. Lett.* **122**, 086402 (2019).
- [30] T. Devakul, V. Crépel, Y. Zhang, and L. Fu, Magic in twisted transition metal dichalcogenide bilayers, *Nature Commun.* **12**, 6730 (2021).
- [31] See Supplemental Materials for notes regarding continuum model Hamiltonian, moiré band structures, DFT calculations, LDA band structures, and effective Hamiltonian of the magnetic point group  $6'_{mm'}$ .
- [32] L. Fu and C. L. Kane, Topological insulators with inversion symmetry, *Phys. Rev. B* **76**, 045302 (2007).
- [33] Q.-X. Lv, Y.-X. Du, Z.-T. Liang, H.-Z. Liu, J.-H. Liang, L.-Q. Chen, L.-M. Zhou, S.-C. Zhang, D.-W. Zhang, B.-Q. Ai, H. Yan, and S.-L. Zhu, Measurement of spin chern numbers in quantum simulated topological insulators, *Phys. Rev. Lett.* **127**, 136802 (2021).
- [34] N. Hao and J. Hu, Topological phases in the single-layer FeSe, *Phys. Rev. X* **4**, 031053 (2014).
- [35] A. Luo, Z. Song, and G. Xu, Fragile topological band in the checkerboard antiferromagnetic monolayer FeSe, *npj Comput. Mater.* **8**, 26 (2022).
- [36] In FeSe, the exchange splitting reaches 2-3 eV (also noted in Ref. 35), which significantly exceeds the SOC strength of approximately 0.3 eV. Within the context of spin  $U(1)$  quasi-symmetry, such a large exchange splitting further promotes a nearly quantized SHC value and a small edge gap.